Formation of different types of paramagnetic centers in the alanine dosimeters exposed to alpha and gamma radiation - Study by EPR spectroscopy

Alexandre I Ivannikov, A.M. M Khailov, S.P. P Orlenko, Valeriy F Stepanenko, Francois Trompier, Kassym Sh Zhumadilov

Journal Pre-proof

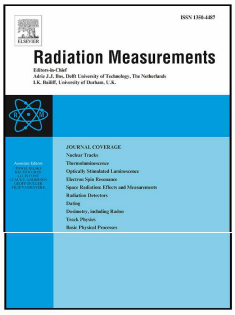

Formation of different types of paramagnetic centers in the alanine dosimeters exposed to alpha and gamma radiation - Study by EPR spectroscopy

A.I. Ivannikov, A.M. Khailov, S.P. Orlenko, V.F. Stepanenko, F. Trompier, K. Sh Zhumadilov

PII: S1350-4487(20)30245-6

DOI: https://doi.org/10.1016/j.radmeas.2020.106467

Reference: RM 106467

To appear in: *Radiation Measurements*

Received Date: 5 June 2020

Revised Date: 8 September 2020

Accepted Date: 17 September 2020

Please cite this article as: Ivannikov, A.I., Khailov, A.M., Orlenko, S.P., Stepanenko, V.F., Trompier, F., Zhumadilov, K.S., Formation of different types of paramagnetic centers in the alanine dosimeters exposed to alpha and gamma radiation - Study by EPR spectroscopy, *Radiation Measurements* (2020), doi: https://doi.org/10.1016/j.radmeas.2020.106467.

Formation of different types of paramagnetic centers in the alanine dosimeters exposed to alpha and gamma radiation - study by EPR spectroscopy

Ivannikov A.I.[a]*, Khailov A.M.[a], Orlenko S.P.[a], Stepanenko V.F.[a],
Trompier F.[b], Zhumadilov K.Sh.[c].

[a] A.F. Tsyb Medical Radiological Research Center, Obninsk, Russia
[b] Institut de Radioprotection et de Surete Nucleaire, Fontenay- aux-Roses, France
[c] L.N. Gumilyov Eurasian National University, Nur-Sultan, Kazakhstan

Keywords: EPR dosimetry, alanine dosimeter, ionizing radiation, paramagnetic centers, spectra decomposition.
* Correspondent author: Alexander I. Ivannikov; E-mail: ivann@mail.ru
tel. +7 48439 97034, fax: +7 495 9561440

Highlights

Different ratio of the EPR spectral components corresponding to different types of radiation induced stable radicals was observed for the alanine dosimeters irradiated by alpha particles and by gamma rays

The observed effect may be used for discrimination of contribution of low and high LET ionizing radiation in mixed radiation field.

Abstract

EPR spectra of alanine dosimeters irradiated by gamma-rays and by alpha-particles were measured at different microwave power. The spectra were decomposed into three components corresponding to different stable radiation-induced radicals. Different ratio of the components was obtained for gamma- and alpha-irradiated alanine. The observed effect can be used for discrimination of the contribution of alpha- and gamma-radiation in mixed radiation field. That may be useful for control of dose at phantom experiments with neutron boron capture therapy, performed in mixed neutron-gamma field in which alpha-particles are emitted through neutrons capture reaction with boron.

1. Introduction

Dosimetric system based on the measurement of EPR spectra of irradiated alpha-alanine is used in various fields (ISO, 2013). The elemental composition of alanine is close to the biological tissue, so its use is recommended in dose control in radiotherapy (Baffa and Kinoshita 2014). There are a large number of studies on the dosimetric properties of alanine dosimeters (AD) for different types of radiation - photons, electrons, neutrons, protons and accelerated ions of different energy (Olssen et al., 1989; Shraube et al., 1989; Hansen and Olsen, 1989). In these studies, dose in the irradiated AD (IAD) was determined related to the signal intensity, which was evaluated by the peak-to-peak amplitude of the central line or by the second integral of the spectrum. Generally, variation of the shape of the spectra for different types of radiation and for different dose levels was considered as not significant and was not taken into account at dose determination.

In fact, the shape of spectra of IAD is changed for different kinds of radiation. Comparative study of the spectrum shape of IAD after exposure to different types of radiation and accelerated ions was carried out in the works (Ciesielski and Wielopolski, 1994, 1995; Ciesielski et al., 1998). The shape of the spectra was characterized by ratio of amplitudes of the two central lines of the spectrum, denoted as Y (narrow line) and X (broader line). It was shown that the ratio of theirs amplitudes, denoted as X/Y, depends on the type of radiation and on the microwave power in the EPR probe cavity. It was shown that X/Y is reduced at irradiation with higher linear energy transfer (LET) relatively to the gamma-irradiation and increased with increasing mw power. No proved and

convincing explanation of this effect was proposed in these publications. The reduction ofX/Y for

the analyzed radiation relatively to the gamma-radiation was characterized by parameter *S*, defined as a slope of observed linear dependence of X/Y for the analyzed radiation relatively to this ratio for gamma-radiation measured at different mw power. The parameter *S* was estimated in for AD exposed to different types of radiation. The value of *S* is changed from 1.0 for ^{137}Cs gamma radiation and 6.6 MeV x-ray (LET=0.3 keVμm^{-1}) to 0.80 for 2.5 MeV protons (LET=20 keV μm^{-1}), 0.85 for reactor's neutrons mixture of fast and thermal neutrons (LET=30 keV μm^{-1}), 0.68 for 1.5 MeV alpha-particles and 0.84 MeV lithium ions, emitted at the reaction of neutrons with boron (^{10}B *(n, α)* ^{7}Li) (LET=250 keV μm^{-1}), and 0.50 for 108 MeV ferric ions (LET=7000 keVμm^{-1}).

Later, it has been shown (Sagusten et al., 1997; Heydari et al., 2002; Malinen et al., 2003) that the spectrum of AD after X-ray irradiation consists of a superposition of the three spectral components corresponding to different types of radicals. The authors of these publications proposed possible structures of these radicals and based on that developed spectra using simulation with spectral parameters described in (10-Heydari et al., 2002). These simulated spectra are presented in **Fig. 1**. For decomposition of experimental spectra to the components, the authors used the linear least square fit procedure, which adjusts magnitudes of the simulated components to the experimental spectrum. This procedure gives possibility to fit only the magnitudes of the components. Therefore, before fitting, it was necessary to align and scale in width the experimental spectra with the model spectra by a special processing using an exact measured value of mw frequency.

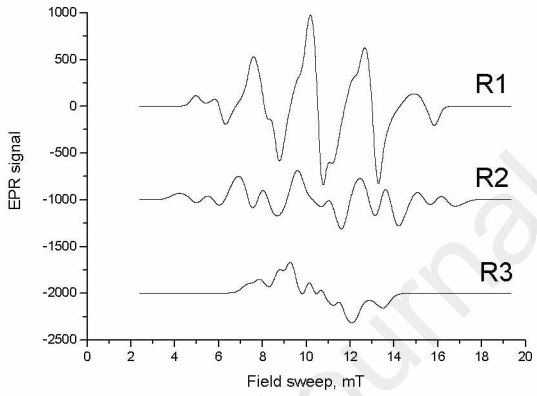

Fig. 1. Simulated components of the EPR spectrum of IAD used for spectra decomposition (Heidari et al.,2002; Malinen et al., 2003). Spectra are centered at *g*=2.0023 and normalized to have the same absorption line area defined by the second integral.

As it is proposed in (Heydari et al., 2002; Malinen et al., 2003), the first type of radical (R1) is formed by deamination of the alanine molecule. The second type of radical (R2) is formed by deprotonation from the central carbon. For the third radical (R3), an unambiguous assignment has not been made, as it is stated in (Heydari et al., 2002). As a possible candidate for this radical a structure was suggested with the oxygen radical in the carboxyl group and the double bond between the central carbon and the carbon of carboxyl group. Change in the spectral shape of IAD at different mw power was explained by different saturation of the spectral components related to different radicals. Dose response of the total spectral amplitude measured as peak-to peak of the central resonance line is linear in the region up to 5-10 kGy. No systematic change of relative contribution of the components over 5-10% was observed in a dose range up to 60 kGy. It was also shown that the relative contribution of the components is changed at heating. After heating at about 200^{o}C, R1 almost disappears, relative contribution of R3 significantly increases, and R2 increased, but not so significantly. In the recent publication (Jastad et al., 2017) modified spectra of the components were proposed with broadened lines taking into account effects of mw power saturation in order to improve fitting.

The simulated spectra developed in (Heydari et al., 2002) were used to decompose the spectrum of AD exposed to x-rays into the three components in the study of effects of visible light illumination on IAD (Ciesielski et al., 2004, 2008). The spectra were decomposed by the same way as in (Heydari et al., 2002). It was shown that at exposure to visible light of the gamma-irradiated AD (gamma- IAD), relative contribution of R1 decreased, R2 increased and R3 did not changed significantly. At storage in darkness during over one year, all components did not change significantly.

Also, it was shown (Ciesielski et al., 2008), that for AD of different manufactures prepared in the form of powder, pills or films with different binder, the ratio of components in the AD irradiated by photons essentially differed. Probably, this effect depends on the microstructure of alanine powder particles and interaction with binder material.

From the observed change in the spectrum shape of IAD characterized by X/Y ratio, contribution of neutrons and gamma-radiation to the total dose after exposure in a nuclear reactor was estimated (Choi et al., 2010). Decomposition of the spectra to the components was not used.

It is reasonably to suppose that change of the spectrum shape and of the X/Y ratio for the different types of radiation is caused by variation of the radical's ratio. However, contribution of the different radicals to the spectra of AD at irradiation with low and high LET was not still examined and no explanation of the effect of differences in X/Y at different types of radiation was proposed.

The purpose of the present work is to analyze the difference in the EPR spectra shape of AD at exposure to radiation with low and high LET (gamma rays and alpha particles respectively) by decomposition of the spectra to the components corresponding to the different types of radicals. It is necessary for development of methods to estimate the contributions of different types of radiation in the mixed radiation fields.

At previous preliminary study (Ivannikov et al., 2016) the effect of decreasing of the ratio of R2/R1 components and increasing of the R3 component at irradiation by alpha-particles (AP) relatively to gamma irradiation was observed in the spectra of alpha-irradiated AD (alpha-IAD) in comparison with gamma-IAD. However, irradiation of AD by AP was performed in the form of pellet exposed with very high local surface dose about 30 kGy, where effects of dose saturation may take place. The pellet of AD was placed by its flat side on the source of AP and exposed for long time in order to obtain sufficiently high signal for detection with average dose about 100 Gy. In the present work we studied AD in the form of powder, which is irradiated by AP more effectively and obtained local dose comparable with dose of gamma-radiation in the range where effects of saturation are excluded.

2. Materials and methods

2.1 Samples preparation and irradiation

Alanine pellet dosimeters (*ES 200-2106, Bruker Biospin)* were used (mass 64.5±0.5 mg,). These AD dosimeters consist of L-α-alanine powder and 4% polyethylene as binder (Bartonicek et al., 2014). The pellets were crushed in a mortar to obtain powder with grain size in the range of 0.1-0.3 mm. The powder was used in order to increase affectivity of alpha irradiation because of its low penetration depth. Both for gamma and alpha irradiation the samples were used in the form of powder prepared from the same batch of alanine pellets. Gamma irradiation of AD was performed with a certified ^{60}Co gamma source at dose 100 Gy in terms of absorbed dose in water with dose rate 10 Gy·min^{-1} and relative uncertainty about 3%. The samples were irradiated in plastic containers, which creating the secondary electron equilibrium conditions.

Irradiation by AP was performed with a source (manufacturer *"Isotope"*, Russia) constructed of a glazier layer about 0.1 mm thickness containing ^{239}Pu coating a steel plate 60·x 26 mm^2 size. The ^{239}Pu emits only alpha radiation with maximal energy of about 5.14 MeV. Flux measurement of AP was performed by a radiometer *MKS-01R-57* (manufacturer *"Baltiets, PB-2335"*, Russia) calibrated using a standard reference source consisting of a surface coated by a thin layer of ^{239}Pu. Measurement was performed through a collimator in the form of cylindrical hole of 2 mm diameter in a brass plate of 1 mm thickness placed on the source surface. The total flux density of AP from

the source was estimated as 7.8-106 cm-2 min-1.

In order to estimate absorbed dose in AD taking into account angle and energy distribution of AP caused byscattering and absorption of AP in the glazier layer of the source, Monte Carlo simulation of the ionizing particle transport was performed using *MCNP-X 2.3.0* code (*Los Alamos Laboratory*) (RSICC, 2002). The details and results of calculations are presented in the previous publication (Khailov et al., 2016). Energy spectrum of AP near a surface of the source and profile of absorbed dose rate in AD layer adjacent to the source is presented in **Fig. 2**.

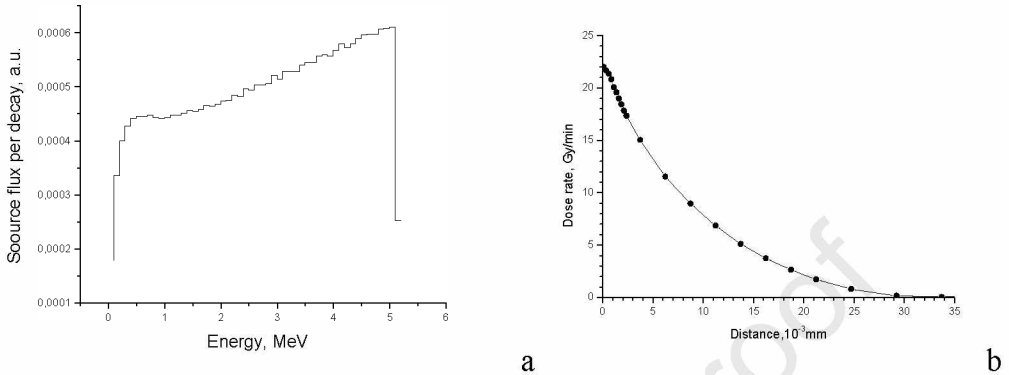

Fig.2. Energy spectrum of AP near a surface of the source (a) and profile of absorbed dose in AD layer adjacent to the source (b) (Khailov et al., 2016).

Because of the scattering and absorption in the glazier layer, a wide energy spectrum of AP appears with average energy 2.83 MeV. Absorbed dose rate at the surface of AD adjacent to the source was estimated by 22 Gy·min^{-1}. According to the calculated dose rate profile, integral dose rate in AD in the form of layer adjacent to the source through the distance from the source is 0.20 Gy·min^{-1}·mm. Average dose rate in AD may be estimated by dividing this value by the thickness of the layer.

At irradiation by AP, the powder of AD with mass about 60 mg was spread on the surface of the source by a thin layer. During exposure, the powder was stirred by a spatula in order to obtain a more uniform irradiation. Exposure was performed during 12 min. At the estimated surface dose rate of 22 Gy·min^{-1}, maximal dose at the surface of the powder particles corresponds to about 264 Gy. In fact, the surface doses are smaller because the powder was stirred during exposure and its particles are irradiated from different sides.

Based on the results of calculation of the dose rate profile, average dose in the irradiated powder may be estimated accepting that the powder consists of grains of cubic form with average size of 0.2 mm spread on the surface of the source by a dense monolayer, and neglect effects of irradiation of the lateral sides of grains. In this case dose rate averaged over the volume of the powder may be determined by dividing of the integral dose rate through its profile by the average thickness of the layer, which is equal to the average grain size. Taking the estimated integral dose rate 0.20 Gy·mm^{-1}·min^{-1} and at the layer thickness 0.20 mm, this average dose rate appeared to be 1.0 Gy·min^{-1}. Thus, total dose at exposure during 12 min is 12 Gy. This is rough value, more exact dose estimation could not be performed because of that the distribution of the shape and sizes of powder's particles was not possible to estimate and take into account.

2.2 EPR spectra measurements and spectra processing

A *Bruker ESP-300E* EPR spectrometer operating in *X*-band and equipped with a TMH resonator cavity was used for measurements. Registration parameters were the following: microwave frequency 9.82 GHz, center field 349 mT, field sweep 20 mT, sweep time 80 s, modulation amplitude 0.1 mT. Spectra measurements were performed at different microwave power

in the range from 0.5 to 64 mW for the reason to demonstrate the difference in the shape of spectra, which is much clear at higher mw power.

Six samples were used for measurement – three samples after gamma irradiation and three samples after alpha irradiation. Mass of each samples was controlled after placement to the probe tube in order to normalize results obtained based on the spectra amplitude measurements to the same sample mass of 60 mg. For gamma-IAD (dose 100 Gy), one spectra accumulation was applied, for alpha-IAD (estimated dose 12 Gy), 16 accumulations were performed.

For the two samples, each after gamma and alpha irradiation, the spectra were measured at different time after exposure at several values of mw power. Between measurements, the samples were stored in a dark place in closed tubes in ambient room conditions. One day after irradiation, when the spectra are stabilized after aging, measurements were performed for all six samples – the three samples after gamma irradiation and the three samples after alpha irradiation.

For the analysis and processing of the spectra of IAD, a computer program was used created in the language *Visual Basic* (*Microsoft*). It was based on the early developed program, which uses the nonlinear least-squares method with Marquard-Levenberg modification (Marquardt, 1965) to fit an experimental spectrum by a simulated spectrum in analytical form and used for dose determination in tooth enamel (Ivannikov et al., 2001, 2010). For decomposition of the spectra of IAD into three components, the program was modified to fit the experimental spectrum by sum of three components presented in numerical form.

The spectra of the components obtained by the EPR spectra simulation of the three types of radiation-induced radicals (**Fig. 1**) accordingly to (Heidari et al., 2002; Malinen et al., 2003) were kindly provided by their authors. The components were normalized to have the same absorption line area obtained by double integration. The authors did not give information about frequency, for which simulation was performed. However, as it follows from the publication (Heidari et al., 2002; Jastad et al., 2017), the experimental spectra for processing of which the simulated spectra were used, were measured with center field 347.5 mT, which corresponds at g=2.0023, the center of the simulated spectra, to mw frequency 9738 MHz. Therefore, it may be supposed that the spectra are simulated for these conditions. In our case, another center field and frequency were used. Therefore it was necessary to adjust center field and spectrum width for performing fitting. Such adjustment was performed in the process of nonlinear fitting. The same modeled spectra of components were used for fitting the experimental spectra measured at different mw power. At fitting, the model spectra were shifted by about 0.3-0.5 mT and their width was increased by about 1-2% as result of adjusting the field position and the width of spectra.

The derivatives of numerical functions describing the components, which are necessary to realize the nonlinear least-squares method, were determined by digital differentiation. At fitting, the following parameters can vary: the height of the baseline (*Vert.offset*), magnitudes of the components (*r1, r2, r3*), shift and width of the total spectrum (*sh1, width*). Possibility is also provided to fit relative shifts between the first component and the two other components (*sh12, sh13*). Novelty of the developed and applied method of fitting was the ability to fit not only the magnitudes of spectrum components as it was done in the previous works, which used the linear regression method (Heydari et al., 2002; Malinen et al., 2003; Ciesielsky et al., 2004, 2008), but also the field position of the model spectrum and its width, and adjust field shifts of all components. This approach leads to more accurate fitting of the model spectrum, because the spectra components are obtained by simulation based on some assumptions and do not describe exactly the real spectrum. Fitting of the field position and the width of spectra allows for adjustment of the spectra in the horizontal axis, which is necessary at accounting for a specific resonance frequency of a probe cavity. Since variation of the field shift and width of spectra at fitting are possible, no need to perform field positioning and extension of the spectra before fitting to coincide with the modeled spectrum. Such procedure needs exact values of field and frequency, for which additional equipment for the spectrometer is necessary. As result of spectra processing, the contribution of each component is obtained expressed in relative units, defined by the program from the amplitude of the experimental spectrum.

For estimation of the quality of fitting, a relative residual sum of squares after fitting (Ra) and the Pierson regression factor (R_c) were calculated according to the following equations:

$$R_a = [<(y_i - y'_i)^2) > / < (y_i - < y_i >)^2>]^{1/2}; \quad (1)$$

$$R_c = < (y_i - < y_i>)(y'_i - < y'_i >)>/[(< (y_i - < y_i >)^2>< (y'_i - < y'_i >)^2>)]^{1/2} \quad (2)$$

Where: y_i – experimental spectrum amplitude values; i – their indexes; y'_i - calculated spectrum amplitude values after fitting; < > - averaging over all spectrum data values.

The regression factor *Rc* was calculated in order to compare with results of fitting in the other works (Heydari et al., 2002; Malinen et al., 2003) produced by the *MS Excel 2000* at fitting procedure. However, we consider that it is clearer to demonstrate the quality of fitting by the parameter R_a, since it estimates directly the discrepancy between the fitted and experimental spectra by the residual sum normalized by mean squared amplitude reduced by its average value. This parameter is similar to the lack of fit (LOF) parameter used in (Jastad et al., 2017) to characterize difference between the original experimental spectrum and the fitted model spectrum of IAD. The only difference is that when calculating LOF, the residual sum is normalized by the mean square amplitude without subtracting its average value.

Uncertainties of the magnitudes of components obtained at execution of the fitting procedure were estimated based on the residual sum and diagonal values of the least square fit matrix (Richter et al., 1995). These values coincided and in some case (at high mw power) even oversized the mean square scattering of the results obtained at repeated spectra measurements and spectra processing for the same sample.

3. Results and discussion

3.1 Spectra of AD at different microwave power after gamma and alpha irradiations

Examples of the spectra of gamma- and alpha-IAD recorded at different microwave power since one day after irradiation are presented in **Fig. 3**. It is seen that at low power difference between the spectra shape after gamma and alpha irradiation is hardly noticeable. Although it is possible to note some difference between at 346 and 347 mT, where a peak appears, which is more intensive for gamma IAD. This peak corresponds to the peak at 5.0 mT of the simulated spectrum of R2 **(Fig. 1)**. At higher power, the difference between the spectra shape become much more prominent. The amplitude of the central narrow line with peaks marked as Y decreased relatively to the central wider line peaks marked as X. The most difference is observed in the central part of the spectra at 40 mW power, where the maxima of the two central lines for gamma- and alpha-IAD inverted by their amplitudes. Such inversion occurs between 10 and 20 mW for gamma-IAD, and between 40 and 64 mW for alpha-IAD.

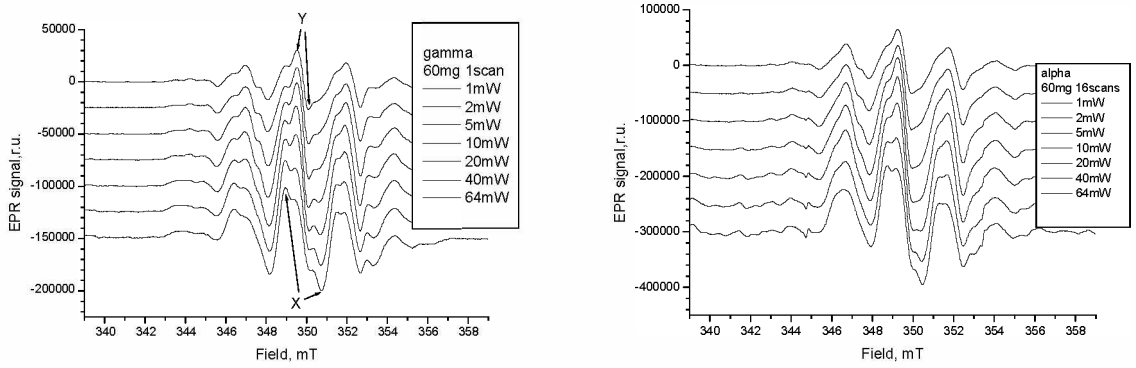

b a b

Fig. 3. Comparison of EPR spectra of gamma IAD (a) and alpha-IAD (b) recorded at different microwave power. Microwave power values, sample mass and number of accumulations are shown on the inserts in the plot panels. The central narrow line is denoted by Y, the central

wider line is denoted by X. Two narrow lines at about 345 and 353 mT of low intensity revealed high power are caused by a MnO reference sample mounted in the cavity.

This effect of the reduction of the mw power value, at which such inversion of the central lines amplitudes relatively to the spectra of gamma-IAD occurs, may serve as indicator of the exposure to alpha radiation. In the mixed radiation field, in which both alpha and gamma radiation is presented, spectra induced by alpha and gamma radiation are superimposed, and such shift will be observed, however at lower mw field values than for the pure alpha radiation. The similar effect also is expected at presence of other kinds of radiation with LET higher than that for gamma radiation.

By the point of inversion of the amplitudes of X and Y components obtained from the measurements at different mw power, the presence of radiation exposure with increased LET can be qualitatively determined. The greater the power corresponding to the inversion point then the greater the contribution of the densely ionizing radiation.

Dose in alpha-IAD may be estimated independently from the amplitude of its spectrum by comparing with the amplitude of the spectra of gamma-IAD. Peak-to-peak maximal amplitude for gamma-IAD measured at 1 mW is 56,500 r.u., for alpha-IAD – 115,300 r.u. From the dose in gamma-IAD of 100 Gy multiplied by the ratio of their amplitudes normalized by the number of spectra accumulations and by the sample mass, dose in alpha-IAD may be estimated, and it appears equal to 12.8 Gy. This dose appears very close to the dose of 12 Gy estimated basing on the intensity of the alpha-source and the dose profile of alpha-radiation in AD in the form of powder despite on very rough assumptions about powder grain sizes.

3.2 Spectra decomposition to the components at different mw power

Examples of the results of spectra processing by the fitting with the simulated spectrum at the two values of mw power are presented in **Fig. 4.** Parameters characterizing quality if fit, *Ra* and *Rc*, calculated according to Equations (1, 2), are presented on the plot panels. It is seen that the simulated fitted spectrum does not perfectly describe the experimental spectrum even at low mw power. This is because of the model components used for composing of the simulated fitted spectrum were calculated with not perfectly exact values of the line width, g-and A-tensors, which were obtained with some assumptions. Increasing of the residual spectrum at higher mw power indicates worsening of the fit. This is because of the shapes of lines composing the experimental spectra are changed due to effects of mw power saturation, but the same modeled benchmark spectra of components are used for fitting. Mainly, at saturation the shape of lines is changed by broadening (Poole, 1967).

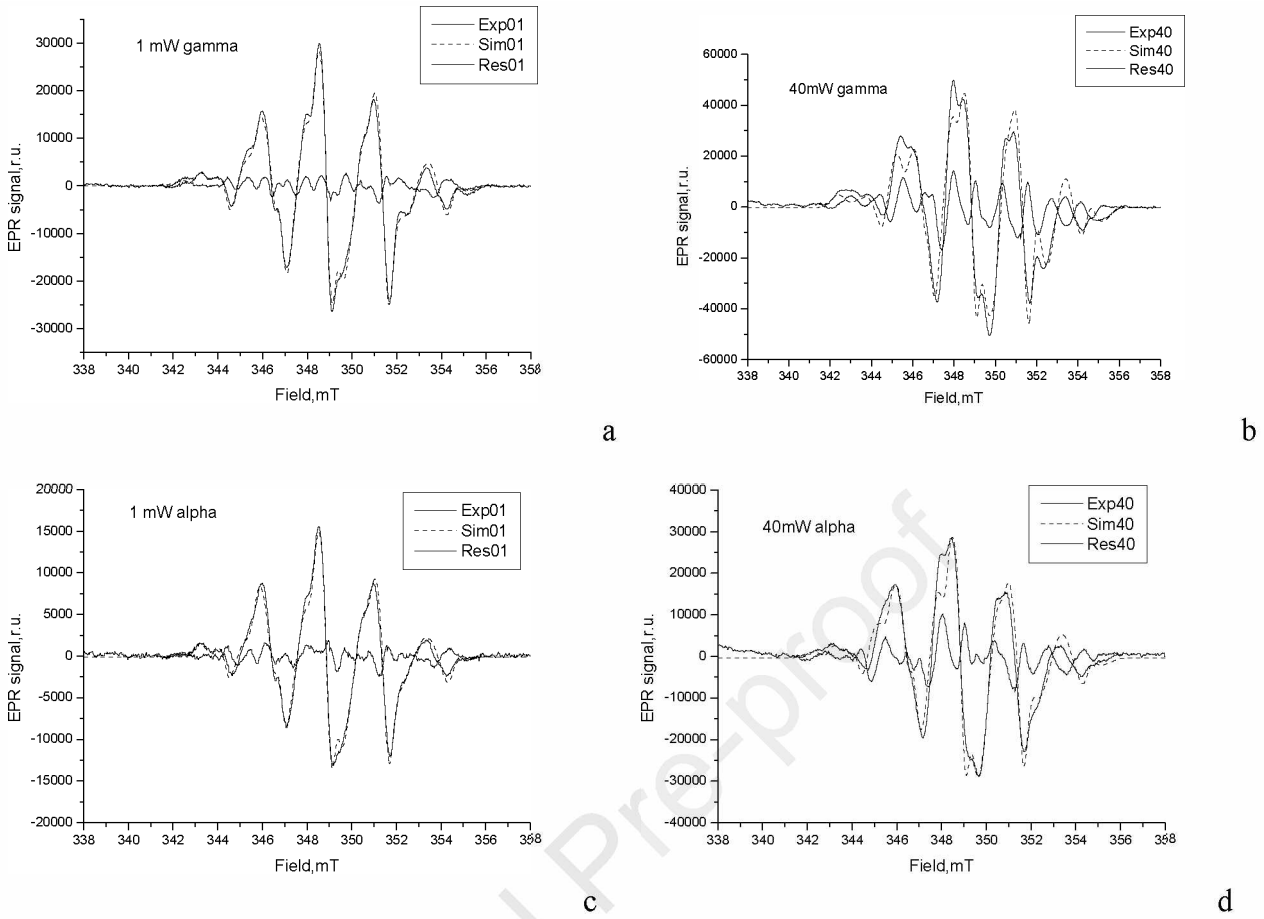

Fig. 4. Examples of the results of spectra processing by the fitting procedure for gamma-IAD (a, b) and alpha-IAD (c, d) at different mw power. Power values are presented on the plot panels. Notations: *Exp* – experimental spectrum, *Sim* – simulated spectrum, *Res* – residual spectrum resulting from the difference between the experimental and the simulated spectrum.

Dependences on the microwave power of *Ra* and *Rc* for gamma- and alpha-IAD are presented in **Fig. 6.** The quality of fitting characterized by *Rc* may be compared with results of publication (Heydari et al., 2002), who used squared values of this factor. For gamma-IAD measured at 0.5 mW we estimated $R_c = 0.995$. In (Heydari et al., 2002) decomposition to the same three components was used by linear regression for the spectra of AD irradiated by x-ray to 30 kGy registered also at 0.5 mW power, and the value of $R_c^2 = 0.980$ is obtained, which corresponds to $Rc = 0.990$. Therefore, the use of the nonlinear least square procedure giving possibility to fit the spectra shift and width results in increasing the quality of fitting. That is because of more exact adjusting of the field position and the width of spectra.

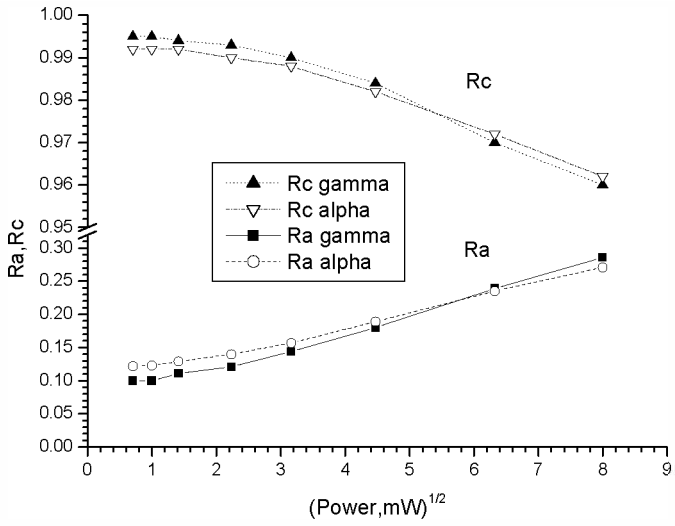

Fig.5. Dependences of the relative residual sum R_a and the correlation factor *Rc* characterizing quality of fitting at spectra decomposition on the mw power for the spectra of gamma- and alpha-IAD.

For alpha-IAD, at low mw power R_a is higher than that parameter for gamma-IAD. For R_c, also worse values are observed for alpha-IAD. This is due to the fact that for alpha-IAD the smaller average irradiation dose was applied. Respectively, smaller EPR signal was observed with higher relative contribution of the spectrometer's low frequency noises caused by distortion of its base line. At higher mw power, *Ra* and *Rc* indicate better fit for alpha-IAD than that for gamma-IAD. This is probably because of the spectrum of alpha-IAD contains higher contribution of lower saturated components than the spectrum of gamma-IAD.

3.3 Analysis of the power dependences of the components

Dependences of the magnitudes of components of the spectra of gamma- and alpha-IAD on mw power obtained as a result of spectra decomposition are shown in **Fig. 6.** These results are based on the spectra measured for the three samples each for alpha and gamma IAD after aging one day after irradiation. The component's values are obtained by averaging results of repeated measurements of the three samples and their uncertainty is obtained as combination (root of the sum of squares) of the uncertainty of the average and the uncertainty given by the fit. The relative amplitudes are defined as a ratio of component's magnitudes to the sum of all three components.

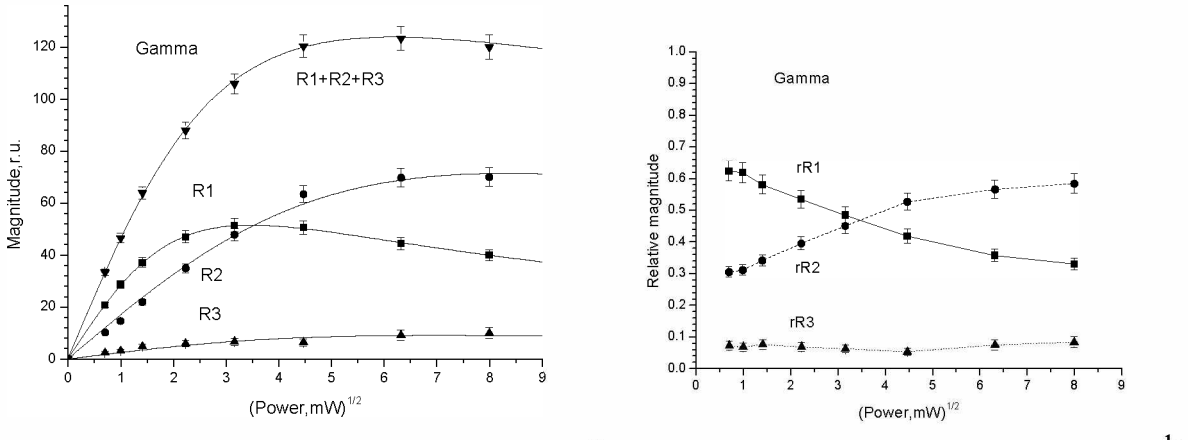

a b

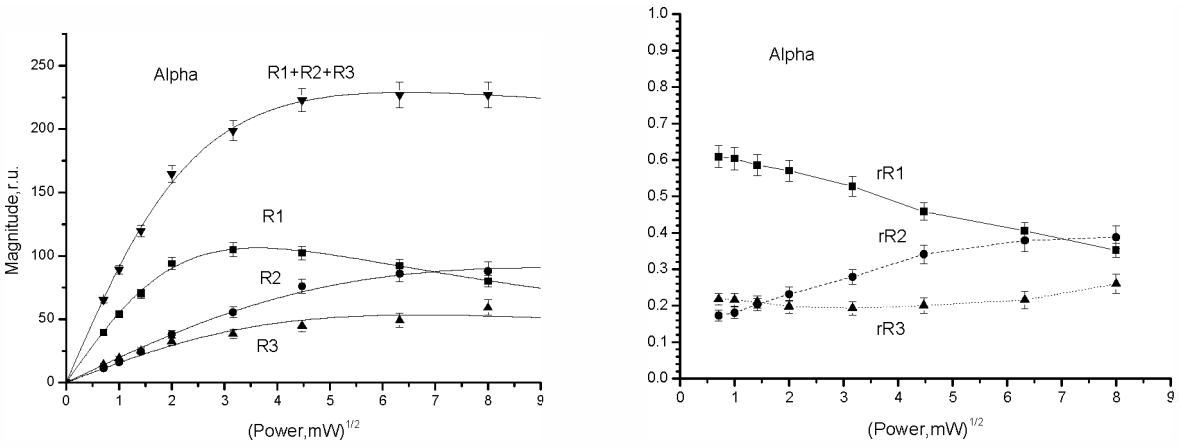

c d

Fig.6. Results of decomposition of EPR spectra of IAD to the three components in dependence on the microwave power: (a, b) - after gamma irradiation; (c, d) - after alpha irradiation; (a, c) - for the magnitudes of components and their sum; (b, d) - for the relative magnitudes of components normalized by their sum. The data points in (a, c) are joined by curves obtained according to Equation (3) with parameters given in Table 1

Intensity of each model component estimated by the second integral is normalized to the same value. Therefore magnitudes of each component in **Fig 6 a,c** are proportional to the spin number of each component, but only in the mw power range where the saturation effects are negligible, that is in the initial linear parts of the plots. At higher power the magnitudes are declined from the linear dependence because of saturation, different for various components.

The relative magnitudes of components in the initial parts of the plots in **Fig. 6 b,d** at the low level of saturation approximately correspond to the relative numbers of spins for each type of radicals. At higher power, because of effects of saturation, relative magnitude for R1 decreases, for R2 increases. The relative magnitude for R3 is higher for alpha-IAD than that for gamma-IAD and changes insignificantly reflecting that its saturation behavior is close to that for the summary magnitude.

The difference between the spectra of alpha- and gamma-IAD is especially notable at elevated microwave power of registration because of larger power saturation of the signal from R1 radicals, which are produced by gamma radiation at higher relative concentration, than by alpha particles. Therefore the changes in line-shape caused by increasing mw power occur in gamma-IAD earlier (at lower powers), than in alpha-IAD. The difference between power dependencies for the components of gamma- and alpha-IAD **(Fig.6)** may be characterized by mw power value, at which magnitudes of R1 and R2 components are equal. This is about 10 mW for the gamma-IAD and 50 mW for the alpha-IAD. These values correspond to mw power at which inversion of X and Y extremes in the spectrum takes place (**Fig.3**) and explain such inversion.

For the alpha-IAD the power value at which these dependencies intersect, is higher by approximately five times relatively to the intersect power for gamma-IAD. This ratio does not depend on the type of resonator probe cavity used, which defines the local mw strength. For the pure alpha radiation this ratio is about 5, for the mixed alpha-gamma radiation field this ratio should have a smaller value, between 1 and 5. The increasing of this value relatively to the pure gamma irradiation may be used for indication of the presence of radiation with higher LET.

The saturation dependencies of the magnitudes of components, *A(P),* was analyzed by fitting with a function based on that presented in (Poole, 1967):

$$A(P) = A_0 \cdot P^{1/2} \cdot (1 + P / P_{sat})^{-b}, \qquad (3)$$

Where: P – mw power, in mW; A_0, P_{sat} and b - fitted parameters characterizing saturation behavior.

For the component R1 and for the summary magnitude, the power dependence is well fitted by such function. For the components R2 and R3, it appeared not possible to fit the dependences by the function with all three variable parameters. This is because of for these components the saturation power parameter *Psat* is too high to be fitted together with the exponential parameter *b* in the measured power range. Therefore, the dependences for these components were fitted by the function (3) with fixed *b*=1. The parameters obtained at fitting are presented in **Table 1**; the fitted curves are shown on the appropriate plots in **Fig.6 a,c**.

Table 1. Parameters of the functions describing the dependences of the components on mw power according to Equation (3).

Gamma-irradiated AD								
Par.	*R1*	*er*	*R2*	*er*	*R3*	*er*	*Sum*	*er*
A_0	31.1	1.3	17.2	0.6	2.6	0.3	48.5	0.3
Psat	10.2	0.6	69.1	7.1	49	13.1	13.2	1.3
b	0.93	0.02	1	0	1	0	0.71	0.03
Alpha-irradiated AD								
Par.	*R1*	*er*	*R2*	*er*	*R3*	*er*	*Sum*	*er*
A_0	59.0	1.4	19.8	0.7	15.9	1.4	9.6	2.2
Psat	12.6	2.0	84.2	10.4	45.2	10.2	10.8	1.9
b	0.98	0.07	1	0	1	0	0.63	0.04

Notations: er – uncertainty given by the fit.

Differences in the parameters characterizing saturation of R1 for gamma- and alpha-IAD are insignificant, within the uncertainties of their determination, and may be explained by not exact decomposition of the spectrum, which is especially expressed at high mw power. At reduced number of parameters, at fixed *b*=1, for gamma- and alpha-IAD the values *Psat* = 12.3±0.4 and 13.0±1.0, respectively, are obtained for R1 (not shown in Table 1), which are very close. For R2 and R3, difference in *Psat* also insignificant, within the error of their determination. It is follows that saturation behavior of each component is similar both at alpha and gamma irradiation.

In publication (Heydari et al., 2002) the saturation maximum for R1 is observed at 16 mW. In the present work tha saturation maximum is observed at about 10 mW. At comparing this result with the result of (Heydari et al., 2002) it should be taken into account that they used a standard EPR cavity, and in the present work the TMH cavity was used, which has higher quality factor Q. So, at the same applied power, at higher Q local mw field strength in the cavity is higher, and saturation occurs at lower mw power supplied to the cavity.

Even at the lowest power used in the present work, the effects of saturation takes place leading to reducing of the observed component's magnitude. If to take into account that saturation power parameter *Psat* for R1 is about 12 mW, when, according to Equation (3), at 0.5 mW the estimated magnitude of R1 will be reduced by factor of 0.95 because of the saturation. At 1.0 mW the reduction factor for R1 is 0.91. For R2 and R3 such reduction is more negligible because of these components have higher saturation power.

It should be noted that the observed dependences of the component's magnitudes on the mw power have systematic deviations from the true values, especially at high mw power. The obtained dependences of the magnitude of the components on the power do not exactly reflect their true change. That is because at high power the used form of the model components differs significantly from the true form, which is distorted due to saturation effects. At high mw power difference between experimental and modeled spectra becomes significant. It is seen from **Fig. 4** that at high mw power a peak at 348.0 mT (corresponding to the X-line, denoted in **Fig. 3**) and peak at 345.0 mT are underestimated both for alpha- and gamma-IAD. These peaks are responsible for the central maximum of the R2 component at 7.5 mT and the left side maximum at 5.0 mT (**Fig. 1**). Therefore,

the magnitude of R2 is underestimated at high power and the real value of Psat for R2 radicals is expected to be higher in both alpha- and gamma-IAD.

3.4 Time stability of the component's magnitudes

In order to examine stability of the results of spectra decomposition, spectra of alpha- and gamma-IAD were measured at different mw power and processed by decomposition to the components after different time of storage after exposure. Results obtained for the spectra measured at 1.0 mW ate presented in **Fig. 8.** For gamma-and alpha-IAD R1 and R2 components do not significantly change with time (within few percents, the uncertainty of their estimation). For alpha-IAD R3 significantly reduced during the two first hours after exposure (by about 30% of its initial value) and stabilized after one day of storage. For gamma-IAD, decreasing of R3 is also observed within 25% of initial value, but it is less expressed because of the smaller relative magnitude of this component. As a result, total magnitude for gamma-IAD is reduced by about 2-3%, which is consistent with results of other publication (Olsson and Bergstran, 2001). For alpha-IAD total amplitude is reduced by about 10% of its initial value. Since R1 and R2 do not significantly changes at storage both for gamma- and alpha-IAD, their ratio also is not significantly changed. For the spectra measured at another values of mw power the similar effects for the stability of the components were observed. It should be noted that the observed effect of decreasing R3 after irradiation is a preliminary result based on few measurements, and it should be proved by more detailed experiments.

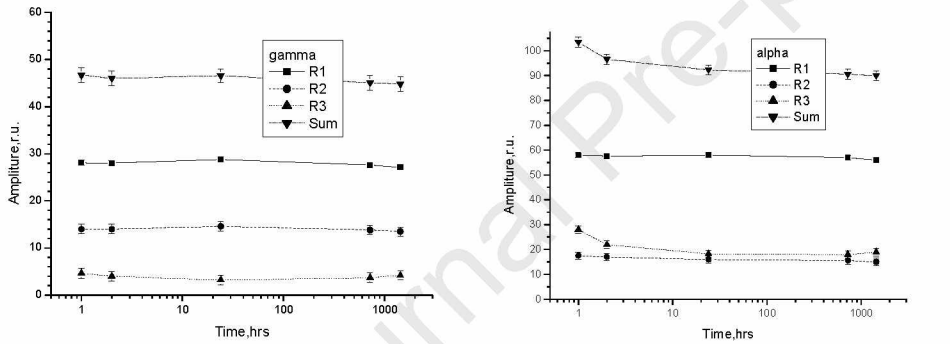

a b

Fig.8. Dependences of the component's magnitudes for gamma-IAD (a) and alpha-IAD (b) on time of storage after exposure. These results arebased on the spectra measured at 1.0 mW.

3.5 Analysis of the ratio of components after gamma- and alpha-irradiation

In order to characterize the difference between spectra of alpha- and gamma-IAD, dependences of the relations between the component's magnitudes R2/R1 on the mw power were examined. These dependencies based on the spectra measured one day after irradiation, are presented in **Fig 9a.** The relation parameter between the ratios R2/R1 for alpha- and gamma-IAD in dependence on the mw power is presented in the same figure. This parameter is defined according to the following equation:

$$S21ag = (R2a / R1a) / (R2g / R1g). \qquad (3a)$$

Where: *R1a, R2a, R1g* and *R2g* – magnitudes of R1 and R2 components for alpha- and gamma- IAD, respectively.

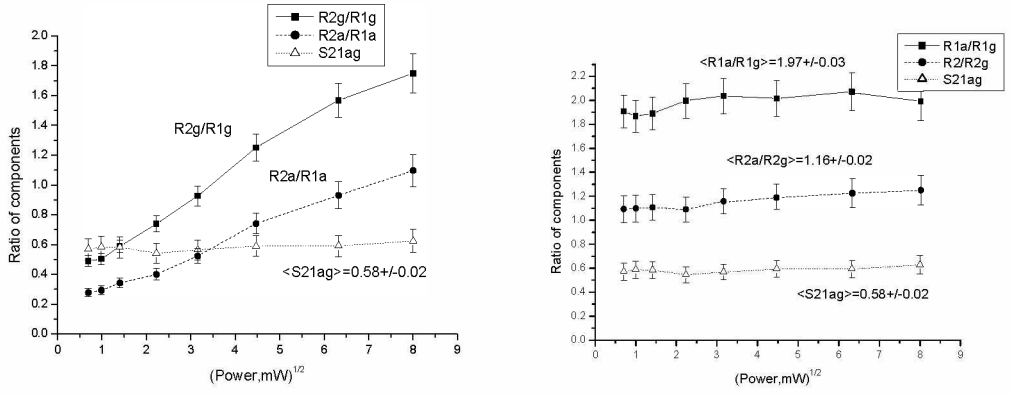

a b

Fig. 9. Dependences of the ratios of the component's magnitudes on the mw power: (a) – the ratios R2/R1 for alpha- and gamma-IAD, and the relation parameter between these ratios *S21ag*. (b) – the ratios of R1 and R2 component's magnitudes for alpha- and gamma-IAD, and *S21ag* determined based on these ratios. These results are based on the spectra measured one day after irradiation. The mean values of parameters shown on the plot panels are obtained as averaged through all values at different mw power.

The ratio R2/R1 is increased with increasing mw power, which is caused by effects of lower saturation of R2 relatively to R1. The uncertainty in R2/R1 increases at higher power because of distortion of the spectra caused by mw power saturation. However the uncertainty of the relation between these values, *S21ag,* almost does not change at increasing mw power.

As it follows from **Fig. 9a**, the parameter *S21ag,* does not exhibit any significant dependence on the mw power, which is explained by that saturation behavior of each component is similar both at alpha and gamma irradiation. Apparently, there is also some systematic error in assessing the magnitudes of components, which is close for each component both for gamma- and alpha-IAD. From the definition of *S21ag* it follows that this parameter is defined by the relation of each type radicals' ratios in alpha- and gamma-IAD, as it is seen from the following equation:

$$S21ag = (R2a/R1a) / (R2g/R1g) = (R2a/R2g) / (R1a/R1g). \quad (3b)$$

Dependences of the ratios of the different component's magnitudes *R1a/R1g* and *R2a/R2g* for alpha-IAD relatively to their magnitudes for gamma-IAD are presented in **Fig. 9b**. These ratios are not significantly changed with mw power. This reflects the fact that the components in alpha- and gamma-IAD have the same saturation behavior and the same systematic errors of their determination, which are compensated for the ratios of components. Determined based on these ratios according to Equation (3b) *S21ag* has the same dependence as in **Fig. 9a** and the same average value.

3.6 Comparison of the results of decomposition to components with the results of estimation X/Y ratio.

In order to compare with results of other authors (Ciesielski et al. 1995, 1998), we have measured dependences of amplitudes of X and Y components of gamma- and alpha-IAD on the mw power. Amplitudes of the X and Y lines were measured as differences between their maximum and minimum at same field positions for spectra measured at different mw power. These positions are well defined by appropriate peaks for the X line at low mw power and at high power for the Y line (**Fig. 3**). Based on the measured amplitudes, we determined X/Y ratio parameters for both kinds of irradiation.

Dependence of the X/Y ratio for alpha-IAD versus the X/Y ratio for gamma-IAD is presented in **Fig 10a.** The linear regression slope of this dependence gives the parameter S = 0.65±0.01. This value is close to the value S = 0.69±0.03 obtained by (Ciesielski et al., 1995, 1998) for the products of nuclear reaction of neutrons with alanine and boron mixture (0.84 MeV lithium ions and 1.5 MeV alpha particles).

irradiation) is also presented in **Fig. 10a,** and it is well described by the linear fit. The dependence for R2/R1 ratio is characterized by the slope parameter 0.56±0.01. Its value is close to the parameter *S21ag* determined as the average relation between R2/R1 ratios for alpha- and gamma-IAD (**Fig. 9);** that is because both these parameters have the same meaning, but were determined by different ways.

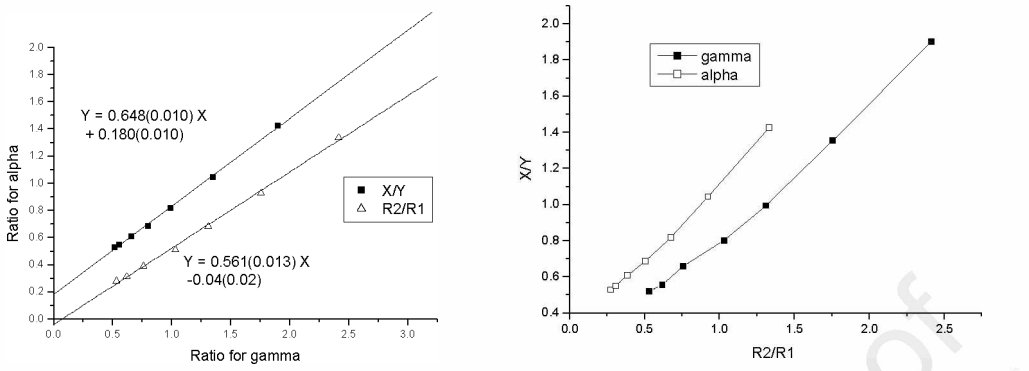

a b

Fig. 10. (a) - Dependencies for X/Y and for R2/R1 measured at different mw power for alpha-IAD versus these parameters measured at the same mw power for gamma-IAD. Parameters of regression lines with uncertainties in the parenthesis are presented in the plot panel. (b) – Relation between X/Y and R2/R1 measured at different mw power for gamma- and alpha-IAD (higher values of X/Y and R2/R1 correspond to higher mw power).

Looking at the shape of simulated spectral components (**Fig. 1**), it may be seen that dominant contribution to the central spectral line of experimental spectrum (Y) is given by the central component of R1, and contribution to the wider line (X) with peaks at 9.5 and 12 mT is mainly given by the central components of R2 and also by a wider central component of R1.

Each value of X/Y can be associated with the value of R2/R1 measured at the same mw power (**Fig. 10b**). Thus, it can be assumed that X/Y is defined by the ratio of the components R2/R1, and the parameter *S*, as well as *S21ag*, is defined by R2/R1. Therefore, for *S21ag* it should be also expected dependence on LET similar to that for the parameter *S* as it was observed in (Ciesielski et al., 1998).

3.7 Use of the ratio of component's magnitudes R2/R1 for estimation of the radiation quality

As it follows from **Fig.9a**, R2/R1 is different for alpha- and gamma-IAD at each value of mw power. This difference can be used to estimate the contributions of alpha- and gamma-radiation to dose in case of mixed radiation fields. A derivation of an equation for such estimation is presented below.

Suppose that an investigated sample is irradiated in mixed radiation field with dose composition of alpha and gamma *Dax* and *Dgx,* respectively, with the same energy spectra and with the same LET as used at calibration with pure alpha and gamma radiation. For this sample, the spectrum is described by R1 and R2 components with magnitudes *Rx1* and *Rx2*, which are determined by the relations:

$$R1x = Dax \cdot Rd1a + Dgx \cdot Rd1g; \quad (4)$$

$$R2x = Dax \cdot Rd2a + Dgx \cdot Rd2g. \quad (5)$$

Where:

R1x and R2x – (in relative units) magnitudes of R1 and R2 components, respectively, for AD irradiated by the investigated radiation.

Dax and *Dgx* (in dose units) – doses of alpha and gamma radiation in the analyzed mixed field.

Rd1a, Rd2a, Rd1g and *Rd2g* (in relative units per dose units) - radiation dose sensitivity of R1 and R2 components to alpha and gamma radiation, respectively. These values may be obtained at calibration using sources of alpha and gamma radiation with known dose rate.

Equations (4) and (5) present a system of two equations, which may be resolved relatively to *Dax* and *Dgx:*

$$Dax = (R1x \cdot Rd2g - R2x \cdot Rd1g) / det \quad (6)$$

$$Dgx = (R2x \cdot Rd1a - R1x1 \cdot Rd2a) / det. \quad (7)$$

Where:

$det = Rd1a \cdot Rd2g - Rd1a \cdot Rd2g$ – determinant of the system of Equations (4, 5).

Basing on the solution of the system of equations (4, 5), the relation between alpha and gamma dose components in the mixed radiation field may be obtained from the following equation:

$$Dax / Dgx = (R1x \cdot Rd2g - R2x \cdot Rd1g) / (R2x \cdot Rd1a - R1x \cdot Rd2a) =$$
$$= Rd1g / Rd1a \cdot (Rd2g/Rd1g - R2x/R1x) / (R2x/R1x - Rd2a/Rd1a). \quad (8)$$

As it follows from (Malinen et al., 2003) relative contributions of R1 and R2 components do not depend significantly on the radiation dose and their magnitudes are proportional to dose (at least in the relative low dose region in the absence of dose saturation). The ratio of dose sensitivity of R2 and R1 components also will not depend on dose and equal to the ratio of components R2/R1 at gamma and alpha irradiation, that is:

$Rd2g / Rd1g = R2g / R1g = S21g$ and $Rd2a / Rd1a = R2a / R1a = S21a$.

The Equation (8) may be rewritten in the following form:

$$Dax / Dgx = K1ga \cdot (S21g - S21x) / (S21x - S21a). \quad (9)$$

Where:

$K1ga = Rd1g / Rd1a$ –parameter depending on the relative sensitivity of the R1 component to gamma and alpha radiation. This parameter is expected not to depend on the mw power and should be determined experimentally at calibration as ratio of R1 components for gamma- and alpha- IAD measured at the same conditions and normalized by radiation dose.

$S21x = R2x / R1x$ - ratio of the amplitudes of R2 and R1 components for the spectra of AD irradiated in the analyzed mixed field.

$S21g = R2g / R1g$ and $S21a = R2a / R1a$ - ratio of R2 and R1 components after gamma and alpha irradiation, respectively.

Equation (9) contains parameters depending on the mw power. To avoid these dependences, it can be converted into the following form:

$$Dax / Dgx = K1ga \cdot (1 - S21xg) / (S21xg - S21ag). \quad (10)$$

Where:

$S21ag = S21a / S21g = (R2a / R1a) / (R2g / R1g)$ – reduction factor of R2/R1 ratio for alpha-IAD relatively to gamma-IAD obtained at calibration for pure alpha and gamma radiation. This factor was already introduced and estimated above, in Section 3.5.

$S21xg = S21x / S21g = (R2x / R1x) / (R2g / R1g)$ – experimental reduction factor used to characterize the investigated radiation.

By using Equation (9), and *S21x*, measured at the same registration conditions, the dose ratio for the investigated mixed radiation field may be estimated. The parameters used in Eq. (9) depend on the mw power (except *K1ga*), and all these parameters should be estimated for the spectra measured at the same registration conditions of mw power.

Based on the results, presented in **Fig. 9,** at mw power 1.0 mW, in conditions of low mw power saturation, $S21g = 0.51 \pm 0.04$ and $S21a = 0.30 \pm 0.03$. In the mixed radiation field containing both gamma and alpha radiation, parameter *S21x* is expected to have an intermediate value.

The parameter $K1ga = (Rd1g1/Rd1a)$ may be estimated based on the results obtained in the present paper for the magnitude of R1 at gamma and alpha irradiation. Based on the results, presented in **Fig. 9,** in conditions with low level power saturation, at 1.0 mW power, $R1a$=54 r.u. with estimated average over the sample dose 12 Gy measured at 16 scans for alpha IAD and $R1g$=29 r.u. and with dose 100 Gy measured at 1 scan for gamma-IAD. at the same conditions and determined in the same relative units. The ratio of these components is 1.87 ± 0.13. After

normalizing of the component' magnitudes by the numbers of scans and by the dose values,

K1ga=0.97±0.06 is obtained. At estimating of the uncertainty of this parameter, only uncertainty of the ratio of components was taken into account, but not the uncertainty in dose estimation.. The main contribution to the uncertainty of this value is defined by the systematic uncertainty of dose estimation for the alpha irradiation, which was estimated quite roughly and it is hard to assess this uncertainty. Based on the average value of *R1a/R1g* = 1.97±0.03, obtained at different mw power, presented on **Fig. 9b**, after normalizing by the doses and by the numbers of scans, the same value of *K1ga*=0.97+/-0.02 is obtained, but with smaller uncertainty.

The parameter *S21ag* does not significantly depends on the mw power as it seen in **Fig. 9,** and after averaging for different mw power it is estimated as *S21ag* = 0.58±0.02. From the measurements performed at 0.5 and at 1.0 mW, a close values, but with higher uncertainty is obtained 0.57±0.07 and 0.58±0.06, respectively. For the investigated radiation, the parameter *S21xg* should be determined as measured at any mw power or as averaged value from the plots similar to that presented in **Fig. 9** for measurements performed at different mw power. Thus, the ratio of doses in the mixed field may be estimated according to Eq. (10) basing on the parameters *S21ag* and *S21xg* determined at any mw power. However, in case of measuring at different mw power the accuracy of this parameter determination may be higher as a result of averaging of the data obtained in multiple different measurement conditions.

In case of pure alpha irradiation, *S21xg* = *S21ag* = 0.58. In case of pure gamma irradiation, *S21xg* = 1, and *Dax / Dgx* = 0. In the intermediate case of mixture of alpha and gamma radiation, *S21xg* is expected to be between 0.58 and 1.0.

The spectrum of AP emitted by the source used for irradiation have broad energy spectrum as it is estimated in (Khailov et al., 2016). At each energy AP are characterized by different LET (Venkataraman et al., 1975). It should be expected that for each fraction of AP with different LET a different ratio of components R2/R1 will be produced. Therefore, the resulting *S21a* value as well as *S21ag* is due to the averaged contribution of various radiation fractions with different LET. This should be taken into account when interpreting data obtained for the investigated mixed fields.

The proposed method can make possible to estimate the contribution of dense and rare ionizing radiation in the mixed radiation field as some resulting dose ratio with respect to the conditions under which the calibration measurements were carried out, in our case, in relation to the alpha radiation of the source used.

In case of presence of other kinds of irradiation in the mixed radiation fields with high LET, such as neutrons, protons and accelerated ions contaminated by gamma, another value of reference ratio of R2/R1 relative to that for gamma radiation is expected, and this value defined analogous to *S21ag* should be experimentally determined to use in the Equation (9) or (10) for determination of the relative contribution of such radiation.

For pure alpha radiation, in conditions of irradiation which is used in the present work, the parameter *S2ag* is estimated by 0.58. For calibration by radiation with a higher LET, the value of *S2ag* is expected to have a lower value. For radiation with a lower LET than that of alpha radiation, the parameter *S2ag* will be greater than 0.58, and in case of using radiation with LET close to that for gamma radiation, it will approach 1.0.

It may be supposed that the reduction factor *S2ag* is specific to the energy distribution of the AP, which may be characterized by some effective value of LET. In case of radiation with energy distribution different from radiation used for calibration, the resulting reduction factor will be caused by some effective LET characterizing this radiation.

Of particular interest is the use of AD for dose control at boron-neutron capture therapy in phantom experiments. As it is known, the main radiation effect of neutron exposure in this case is due to the formation of alpha-particles, recoil ^{7}Li nucleus and secondary gamma radiation at the decay of isotope ^{10}B. The addition of boron compounds (natural isotope content of ^{10}B is 20%) in AD increases its EPR sensitivity, according to various estimates, from 12 (Galindo and Klapp, 2005) to 40 times (Ciesielsky et al., 1995) because of the production of high LET particles. This is of interest to use AD for estimation contributions of different types of radiation to the absorbed dose

at neutron capture therapy in order to assess the biological effectiveness, which may be estimated based on contribution of low and high LET radiation.

4 Conclusion

It is shown that the shape of EPR spectra of AD exposed to alpha- and gamma-radiation is different. This difference is due to the reduced contribution of R2 type radicals relatively to R1 radicals at irradiation with alpha-particles.

The difference between spectra may be characterized by the ratio of spectral components magnitudes R2/ R1. For alpha-radiation, this ratio is smaller relatively to this ratio obtained for gamma-radiation, by factor of 0.58±0.02, and it does not significantly depend on the mw power at EPR spectra measurement. The expression is derived, with the use of which, based on this factor, relative contribution of alpha-radiation to total dose for the mixed alpha-gamma radiation field may be estimated.

However, since a number of authors noted that the ratio of components in IAD changes when exposed to high temperatures (Heidari et al., 2002; Malinen et al., 2003; Jastad et al., 2017) and to intense visible and UV light (Ciesielsky et al., 2004, 2008), the effect of these factors should be monitored and excluded when the samples are irradiated, as well at storage of the samples before measurement.

Acknowledgements

This work is supported by the Russian Foundation of Basic Researches [grant numbers 15-58-45050 IND_a, 16-04-01276 A]; and the Ministry of Education and Science of Kazakhstan [№ AP05135470]. We are very grateful to the research group of E. Sagstuen (M. Heydari, E. Malinen, E. Hole) (University of Oslo) for possibility to use their simulated spectra of components of alanine radicals.

References

Baffa O., Kinoshita A., 2014. Clinical applications of alanine/electron spin resonance dosimetry // Radiat. Environ. Biophys. 53, 233-240.

Bartonicek B., Kucera J., Svetlik I., Viererbl V., Lahodova Z., Tomaskova L., Cabalka M., 2014. Extended use of alanine irradiated in experimental reactor for combined gamma- and neutron-dose assessment by ESR spectroscopy and thermal neutron fluence assessment by measurement of 14C by LSC Applied Radiation and Isotopes 93, 52-36.

Choi H., Kim J., Lee B., Lim Y., 2010. Application of alanine/ESR spectrum shape change in gamma dosimetry. Nuclear Engineering and Technology 42, 313-318.

Ciesielski B Schultka K Penkowski M Sagstuen E, 2004.. EPR study of light illumination effects on radicals in gamma-irradiated L-alanine. Spectrochimia Acta Part A 60, 1321-1333.

Ciesielski B., Tyszkowska M., Grudniewska A., Penkowski M., Schultka K., Peimel-Stuglik Z., 2008. The effect of dose on light-sensitivity of radicals in alanine EPR dosimeters. Spectrochimia Acta Part A 69, 1405-1416.

Ciesielski B., Wielopolski L., 1994. The effects of dose and radiation quality on the shape and power saturation of the EPR signal in alanine. Radiat .Res. 140, 105-111.

Ciesielski B., Welopolski L., 1995. The effects of boron on electron paramagnetic resonance spectra of alanine irradiated with thermal neutrons. Radiat. Res. 144, 59-63.

Ciesielski B., Stuglik Z., Wielopolski L., Zvara I., 1998. The effect of high-linear energy transfer ions on the electron paramagnetic resonance signal induced in alanine. Radiat. Res. 150, 469-474.

Galindo S., Klapp J., 2005. EPR borax-alanine mixtures irradiated with thermal neutrons. Revista Mexicana de Fisica 51, 193-198.

Hansen J.W. and Olsen K.J., 1989. Predicting decay in free-radical concentration in L-a-alanine following high-LET radiation exposures. Appl. Radiat. Isot .40, 935-939.

polycrystalline alanine EPR spectrum studied by ENDOR, thermal annealing and spectrum simulations. J. Phys. Chem. A 106, 8971-8977.

International organization for standardization (ISO), 2013.Radiation Protection - Standard Practice for Use of the Alanine-EPR Dosimetry System ISO 51607. ISO, Geneva.

Ivannikov A.I., Skvortsov V.G., Stepanenko V.F., Tikunov D.D., Takada J., Hoshi M., 2001. EPR tooth enamel dosimetry: optimization of the automated spectra deconvolution routine. Health Phys. 81,124-137.

Ivannikov A., Sanin D., Skvortsov V., Stepanenko V., Tsyb A., Trompier F., Zhumadilov K., Hoshi M., 2010. Dental enamel EPR dosimetry: Comparative testing of the spectra processing methods for determination of the radiation-induced signal amplitude. Health Phys. 98, 345-351.

Ivannikov A.I., Khailov A.M., Skvortsov V.G., Orlenko S.P., Stepanenko V.F., Suriyamurthy N., 2016. A study of characteristics of the formation of stable paramagnetic centers in alanine exposed to alpha radiation by electron paramagnetic resonance spectroscopy. Radiation and Risks 25, 85-93 (*in Russian*).

Jastad E. O., Torheim T., Villeneuve K. M., Kvaal K., Hole E. O., Sagstuen E., Malinen E., Futsaether C. M., 1985. In quest of the alanine R3 radical: multivariate EPR spectral analyses of X-irradiated alanine in the solid state. J. Phys. Chem. A 121, 7139−7147.

Khailov A.M., Ivannikov A.I., Skvortsov V.G., Orlenko S.P., Stepanenko V.F., Suriyamurthy N., 2016. Evaluation of the relative radiation sensitivity of alanine to alpha radiation by electron paramagnetic resonance spectroscopy. Radiation and Risk, 25, 76-84 (*in Russian*).

Malinen E., Heydari M.Z., Sagstuen E., Hole E.O., 2003. Alanine radicals, part 3: properties of the components contributing to the EPR spectrum of X-irradiated alanine dosimeters. Radiat. Res. 159, 23-32.

Marquardt, D., 1963. An algorithm for least-squares estimation of nonlinear parameters, SIAM Journal on Applied Mathematics 11(2), 431–441.

Olsen K.J., Hansen J.W., Waligorski M.P.R., 1989. ESR dosimetry in calibration intercomparisons with high energy photons and electrons. Appl. Radiat. Isot .40, 985-988.

Olsson S., Bergstrand E., 2001. Calibration of alanine dosimeters. ISRN ULi-RAD-R-92-SE, Report 92 2001-10-11. Link¨oping University, Sweden.

Poole Ch.P., 1967, Electron spin resonance. A comprehensive treatise on experimental techniques. Interscience publishers. New York-London-Sidney,.

Richter P. H., 1995. Estimating errors in least-squares fitting. TDA Progress Report 42-122. August 15, 1995, p.107-137.

Radiation Safety Information Computational Center (RSICC), 2002. Computer Code Collection, Report CCC-715, LANL, Los Alamos.

Shraube H., Weitzenegger E., Wieser A., Regulla D., 1989. Fast neutron response of alanine probes Appl. Radiat. Isot. 40, 941-944.

Sagusten E., Hole E.O., Haugedal S.R., Nelson W.H., 1997. Alanine radicals: structure determination by EPR and ENDOR of single crystals X-irradiated at 295 K. J. Chem. Phys. A 101, 9763-9772.

Venkataraman G., Murthy M.S.S., Viswakarma R.R., 1975. Stopping power of some low atomic number materials for alpha particles of energies up to 6 MeV. Health Phys. 28 (4),461-464.